Conference Paper

Parametric Study of a Plunging NACA0012 Airfoil

Emanuel António Rodrigues Camacho, Fernando Manuel da Silva Pereira das Neves, André Resende Rodrigues Silva, and Jorge Manuel Martins Barata

Universidade da Beira Interior

Abstract

Natural flight has always been the source of imagination for the Human being, but reproducing the propulsive systems used by animals is indeed complex. New challenges in today's society have made biomimetics gain a lot of momentum because of the high performance and versatility these systems possess when subjected to the low Reynolds numbers effects. The main objective of the present work is the computational study of the influence of the Reynolds number, frequency and amplitude of the oscillatory movement of a NACA0012 airfoil in the aerodynamic performance for a constant angle of attack over time. The thrust and power coefficients are obtained which together are used to calculate the propulsive efficiency. The simulations were performed using ANSYS Fluent with a RANS approach for Reynolds numbers between 8,500 and 34,000, reduced frequencies between 1 and 5, and Strouhal numbers from 0.1 to 0.4. The aerodynamic parameters were widely explored as well as their interaction, obtaining optimal operational condition zones for the different Reynolds numbers studied.

Keywords: Plunging, Airfoil, CFD, Aerodynamic coefficients, Biomimicry

Corresponding Author:
Emanuel António Rodrigues Camacho
emanuel.camacho@ubi.pt

Received: 26 November 2019
Accepted: 13 May 2020
Published: 2 June 2020

Publishing services provided by Knowledge E

Selection and Peer-review under the responsibility of the ICEUBI2019 Conference Committee.

Nomenclature

U_∞	Velocity	y	Airfoil vertical position
ρ	Density	$\dot{y}$	Airfoil vertical velocity
μ	Dynamic viscosity	Re	Reynolds number
c	Aerodynamic chord	k	Reduced frequency
A	Plunge amplitude	h	Nondimensional amplitude
f	Plunge frequency	St	Strouhal number
T	Period	C_d	Drag coefficient
W	Wake width	C_l	Lift coefficient
α	Angle of attack	C_t	Thrust coefficient
ξ	Airfoil effective trajectory angle	C_P	Power coefficient
x	Airfoil horizontal position	η	Propulsive efficiency

OPEN ACCESS

1. Introduction

When the flapping airfoil/wing mechanism was unveiled as a thrust production system, the scientific community saw the possibility to investigate new aerodynamic phenomena and develop newer systems that could improve substantially the way airplanes fly nowadays, which is still rather conservative [1]. However, in the first part of the 20^{th} Century, very little effort was made in terms of understanding and exploiting the aerodynamics of living beings.

Animals such as insects [2], birds, small fishes, and even the big blue whale are equipped with a spectacular propulsion system that was subjected to natural selection processes over millions of years which inevitably offers a big advantage [3, 4].

Based on the phenomena seen in Nature, micro and nano aerial vehicles with indispensable civil and military applications such as surveillance, espionage, atmospheric weather monitoring, and catastrophe relief purposes [5] are being developed which offer undeniable maneuverability and efficiency at lower length scales. The most advanced MAVs (Micro Aerial Vehicles) related research projects define these vehicles as vehicles with no length, width or height larger than 15cm, as declared in a Defense Advanced Research Projects Agency (DARPA) program [6].

The flapping airfoil was firstly studied by Knoller & Verein [7] and Betz [8] that found that while plunging an airfoil, an effective angle of attack, which changes sinusoidally over time, would be created. As a result, an oscillatory aerodynamic force normal to the relative velocity was generated which could be decomposed in lift and thrust forces as shown in Figure 1.

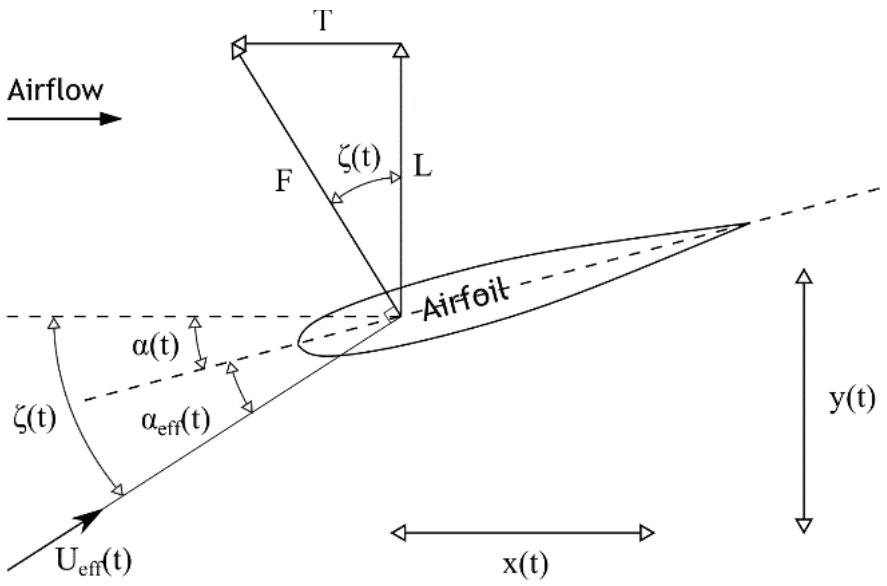

Figure 1: Flapping Airfoil Scheme.

Katzmayr [9] experimentally verified the Knoller-Betz effect in an interesting way, by placing a stationary airfoil into a sinusoidal wind stream and measuring an average thrust. However, the Knoller and Betz theory was only based on the airfoil motion and did not account for the vorticity shed downstream of the airfoil.

Thus, later in 1935, Kármán & Burgers [10] successfully explained theoretically the thrust generation mechanism based on the vortex shedding on the downstream side of the airfoil and the orientation of the wake vortices. They modeled the wake of the flow past bluff bodies at low Reynolds numbers by an infinite row of alternating vortices, commonly known as von Kármán vortex street which is always associated with the production of drag. This typical configuration of wake vortices causes a momentum deficit in the wake compared to the upstream flow and the body experiences drag. This type of wake is commonly referred to as a drag producing wake.

In contrast, the flow past a flapping flat plate or airfoil (pure plunging, pitching or both combined) may produce a wake where vortices induce a velocity or a momentum surplus in the wake compared to the upstream flow which creates a jet-like flow that generates a propulsive force explained by Newton's third law of motion. All these concepts were further studied by Freymuth [11] using flow visualization of both plunging and pitching motions.

Firstly, studying the aerodynamics of plunging and pitching airfoils offered a better understanding regarding the flutter and gust-response effects, which are based only on the analysis of the lifting forces [12, 13]. Oscillating airfoils also opened new ways to study the impact of the dynamic stall on helicopter and propeller blades performance and how impactful is the wake created by a foregoing blade on the following blades [14].

At about the same time as Kármán & Burgers, Garrick [15] applied Theodorsen's inviscid, incompressible, oscillatory, flat-plate theory [16] to the determination of the thrust force and showed that plunging airfoils generate thrust over the whole frequency range and the thrust produced by the airfoil's motion was approximately proportional to the square of kh, whereas pitching airfoils do so only with frequencies above a certain critical value and as a function of the pivot location, for example, an airfoil pitching about a point $0.25c$ from the leading edge, the critical reduced frequency value would be about 3.25. It should be noted that Garrick considered potential flow which does not take into consideration the viscous effects and only represents small amplitude oscillations. Nevertheless, the use of inviscid methods is not absurd when considering a satisfactorily large Reynolds number and reduced angles of attack as suggested by Platzer *et al*. [6].

Flapping airfoils, more specifically plunging airfoils, have been also analyzed by Lai & Platzer [17], Lewin & Haj-Hariri [18] and Young [19], where the wake structures were intensively studied, such as the vortex-pair shedding that represent the transition from the drag producing wake to the thrust producing inverted von Kármán vortex street. Young & Lai [20] concluded that this type of wake structure was caused by the interaction between bluff-body type natural shedding from the trailing edge and the motion of the airfoil.

In 1996, Tuncer & Platzer [21] used a Navier-Stokes code to estimate the thrust force and propulsive efficiency for a flow passing a NACA 0012 undergoing pure plunging motion (for Re = 3 x 10^6). With the same objective as Schmidt [22], these two authors have also studied the flapping/stationary airfoil combination.

Over the following year, Jones & Platzer [23] presented their results using a 2D incompressible unsteady panel method (UPM) to investigate if the effect of varying the airfoil's thickness would have any influence on the flow over different airfoil sections undergoing pure plunging motion. They finally found that this parameter does not have an impactful effect on thrust generation and propulsive efficiency in the range of frequencies (k = 0.01-10) and amplitudes (h = 0.1- 0.4) tested.

Tuncer *et al* [24] using a 2D compressible Navier-Stokes solver studied the flow around an airfoil undergoing pure plunging motion at Re = 10^6. They verified that the maximum achievable thrust depends directly on kh losing this dependency after a critical value where dynamic stall starts occurring due to the weak resistance that a laminar boundary layer has to separate. Additionally, it was argued that for optimal propulsive efficiency, it is advantageous to operate in the low frequency and large amplitude range.

The plunging motion was further investigated by Young & Lai [25, 26] that found the impact of the several parameters governing this problem, especially the Strouhal number which showed that maximum thrust and optimum efficiency take place at the near dynamic stall boundary.

However, for lower Reynolds numbers, the problem becomes more complicated because efficient thrust generation is achieved by shedding from both leading and trailing edges.

Interested in finding which flying conditions animals operate in, Taylor *et al* [27] dedicated their studies to forty two species of birds, bats and insects in cruise flight and verified that these creatures fly within a limited range of Strouhal numbers between 0.2 and 0.4, concluding that this parameter is a possible indicator of the flapping conditions

that provide the most efficient flight, being essential to characterize the flight of several natural flyers, regardless of their scale.

As previously mentioned, the flapping mechanism is typically correlated with thrust production since it can, in some conditions, positively change the wake momentum and because of that, it is important to evaluate not only the generated force but also the propulsive efficiency which is the ratio between the generated power, $-DU_\infty$, and the power supply is given by $-L\dot{y}$. The propulsive efficiency is then defined as

$$\eta = \frac{\overline{C_t} U_\infty}{\overline{C_P}} \tag{1}$$

where

$$\overline{C_t} = -\frac{1}{\Delta t}\int_t^{t+\Delta t} C_d dt \tag{2}$$

and

$$\overline{C_P} = -\frac{1}{\Delta t}\int_t^{t+\Delta t} \dot{y} C_l dt \tag{3}$$

In these two last equations, $\overline{C_t}$ is the mean thrust coefficient, C_d is the drag coefficient, C_l is the lift coefficient and $\overline{C_P}$ is the mean power coefficient.

The present work studied numerically, the flapping airfoil problem, in particular, the plunging motion which has not been yet subjected to sufficiently detailed studies when compared with the combined plunging and pitching. Hence, the present work aims at studying the influence of flight velocity, the motion's frequency, and amplitude to fulfill this gap and help to understand the generation of thrust and what combinations in the operating domain are energetically adequate to a vehicle that uses the flapping mechanism as its mean of motion.

The influence of the mentioned parameters will be evaluated using the typical dimensionless quantities for a flapping airfoil: the reduced frequency, k, the non-dimensional amplitude, h, Strouhal number, and the Reynolds number, shown in Table 1.

TABLE 1: Dimensionless Parameters.

Reynolds Number Re	Reduced Frequency k	Non-dimensional Amplitude h	Strouhal Number St
$Re = \frac{\rho U_\infty c}{\mu}$	$k = \frac{2\pi f c}{U_\infty}$	$h = \frac{A}{c}$	$St = \frac{2fA}{U_\infty} = \frac{\tan(\max a_{eff})}{\pi}$

2. Methodology

The general flapping airfoil problem has been vastly investigated using several CFD methods. In the turbulence modeling field, some authors have studied the effectiveness of some turbulent models in representing the flow characteristics but at the same time, it appears that there is a lack of understanding regarding the influence of turbulence on this subject, since the vast majority of published research assumes the flow around flapping airfoils to be laminar. In the present work, a Reynolds Averaged Navier-Stokes (RANS) formulation was used to predict the effects of turbulence on the aerodynamic performance. The Shear-Stress Transport $k-\omega$ model was selected to access its capability in predicting the flow surrounding a plunging airfoil, since it shows, based on already published work, a superior capability in representing the flow surrounding oscillatory airfoils. The flow field is then obtained by solving the continuity and momentum averaged equations, which can be written in a Cartesian tensor form as

$$\frac{\partial \rho}{\partial t}+\frac{\partial\left(\rho u_i\right)}{\partial x_i}=0 \tag{4}$$

and

$$\frac{\partial\left(\rho u_i\right)}{\partial t}+\frac{\partial\left(\rho u_i u_j\right)}{\partial x_j}=-\frac{\partial p}{\partial x_i}+\frac{\partial}{\partial x_j}\left[\mu\left(\frac{\partial u_i}{\partial x_j}+\frac{\partial u_j}{\partial x_i}-\frac{2}{3}\delta_{ij}\frac{\partial u_l}{\partial x_l}\right)\right]+\frac{\partial\left(-\rho\overline{u_i' u_j'}\right)}{\partial x_j} \tag{5}$$

respectively. In this study, the symmetrical airfoil NACA0012 is being used to simulate the plunging motion and analyze the flow configurations created by it. The airfoil's motion is described by the equation

$$y(t)=A\cos(2\pi f t) \tag{6}$$

and its velocity is given by

$$\dot{y}(t)=-2\pi f A\sin(2\pi f t) \tag{7}$$

where A and f are respectively the motion's amplitude and frequency, respectively.

The whole numerical process was achieved with ANSYS in which includes the DesignModeler, AnsysMeshing and Fluent software. The mesh was designed to have two main zones with an interface separating them. This decision allowed the creation of a structured mesh around the airfoil and an unstructured grid in the airfoil's far-field. Hence, the mesh zone containing the NACA0012 acts as a rigid body that moves with the airfoil, meaning that it is not subjected to any mesh update calculation, a process that would waste computation time. The outside zone is set to be a deformable region with a larger element size that effectively reduces the computational demand.

After the generation process of the mesh, the computational boundaries were treated in order to achieve a valid solution. In this problem, four boundaries needed to be treated, being these the inlet, outlet, upper and lower walls and airfoil. The inlet was subjected to an inlet velocity boundary condition where the flow velocity was prescribed, and information required by the turbulence models was given. On the outlet, the outflow boundary condition was applied, which extrapolates the required information from the interior of the computational domain. The remaining boundaries are walls, although with different characteristics, since the airfoil is treated as a wall where the no-slip condition is imposed and, the upper and lower walls are considered to have no shear stress which removes the boundary layer effects that otherwise would appear.

Due to the unsteady characteristics of this problem and airfoil's harmonic motion, it was imperative to activate the dynamic mesh. Within this feature, two methods were selected, being these the spring-based smoothing method and local remeshing. The first one idealizes the mesh as a network of interconnected springs and allows the mesh to deform due to the airfoil's motion. The local remeshing method ensures that the mesh quality would not degrade over time, by controlling the cells' skewness.

Regarding solution methods, and particularly the spatial discretization, the gradients were evaluated using the Least Squares Cell-Based scheme and the pressure interpolation was made with PRESTO! (PREssure STaggering Option), while the momentum, turbulent kinetic energy, and specific dissipation rate were discretized using the QUICK scheme, which is the fusion of a central differencing scheme and second-order upwind scheme. With respect to the transient formulation and knowing beforehand that the dynamic mesh feature was activated, the first order implicit method was the only scheme available. In terms of pressure correction, the pressure-velocity coupling scheme used is PISO (Pressure-Implicit with Splitting of Operators) that is highly recommended for all transient flow calculations [28].

The solution initialization was achieved using the hybrid initialization feature of Fluent. This initialization is a collection of recipes and boundary interpolation methods which solves the Laplace equation to produce a velocity and pressure field that smoothly connects high- and low-pressure values in the computational domain.

After each initialization, the mesh was adapted to ensure that y^+ was between 0 and 1, since when using a turbulence model, it is fundamental to guarantee that the effects of the flow close to the walls are well represented.

As the airfoil was positioned on the center of the internal zone that corresponds to the absolute zero of the referential, the airfoil would initiate its movement with maximum velocity based on equation 7. Thus, to counteract this effect which substantially reduces

convergence time, the airfoil's motion was subdivided into three segments as shown below.

$$\dot{y}(t) = \begin{cases} A/0.5T, & t \leq 0.5T \\ 0, & 0.5T < t < T \\ -2\pi f A \sin(2\pi f t), & t \geq T \end{cases} \quad (8)$$

where $T = 1/f$. The first segment corresponds to the movement of the airfoil from the origin to the position $y = A$ with constant speed during half of the period. In the other half of the period, the airfoil has zero velocity which contributes to achieve a fast stabilization of the final solution. After this 2^{nd} segment, the airfoil is submitted to the harmonic movement expressed by equation 6.

Due to the boundary conditions, solution initialization and nonlinearity which characterizes the Navier-Stokes equations, it was observed that the flow configuration would stabilize after analyzing at least five periods, always maintaining all residuals below 10^{-3}. The numerical validation started by performing a boundary location, mesh independence (verified for 62469 cells/52394 nodes) and time step independence (verified for 200 points oscillation period) studies with *Re* = 17,000 h = 0.5 and k = 2.5 and, continued with the comparison of preliminary results with those already published on the literature, presented in [26], in order to guarantee that the results were not affected by the numerical formulation.

The processing and analysis of the data were made recurring to scripts developed in C language, whose aim was to obtain the averaged aerodynamic coefficients and propulsive efficiency.

3. Results

This section shows the results concerning the influence of Reynolds number, motion's amplitude, frequency and the Strouhal number on the flapping mechanism. Graphics of thrust and power coefficients, as well as propulsive efficiency, will be shown as functions of relevant parameters. The pure plunging NACA0012 airfoil was firstly tested with a *Re* = 8,500 with $1 \leq k \leq 5$, $0.1 \leq St \leq 0.4$, and h never surpassing 0.5.

In Figure 2, the thrust coefficient is shown in the *kh* plane. In the contour plot, it is noteworthy that the C_t value is growing faster than the Strouhal number with respect to k, a phenomenon that becomes evident for a nondimensional amplitude higher than 0.3. The same behavior is not exhibited by the power coefficient which has its isolines

almost parallel to the ones that represent a constant Strouhal number. Bearing in mind that there is a correspondence between *St* and the maximum angle of attack then there must be an implicit relationship between the required power supply to maintain the oscillatory movement and the maximum effective angle of attack to which the airfoil is subjected.

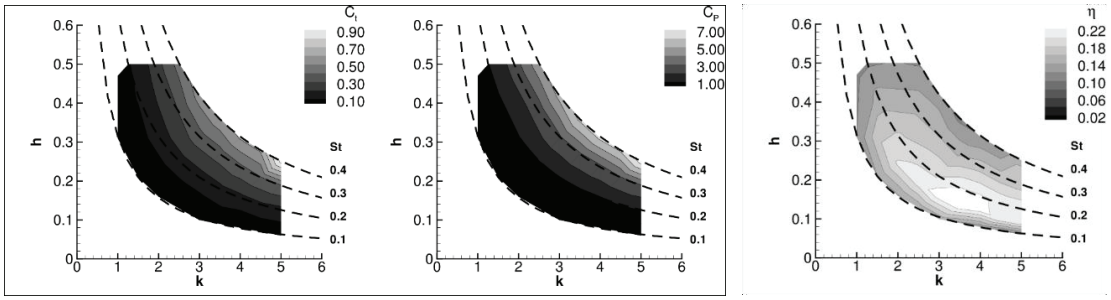

Figure 2: Thrust (C_t) and Power coefficients (C_P) and propulsive efficiency (η) at Re = 8,500.

Regarding the influence of the Strouhal number on the thrust and power coefficients, were obtained the following correlations:

$$C_t(St) = -0.051 + 0.462St + 2.668St^2 \quad (R^2 = 0.87) \tag{9}$$

$$C_P(St) = 0.543 - 8.471St + 52.58St^2 \quad (R^2 = 0.96) \tag{10}$$

with 0.1≤*St*≤0.4. The coefficient of determination of the C_t approximation is under 0.90 which once again reinforces the fact that the isolines of the thrust coefficient are not entirely parallel. The consolidation of C_t and C_P results in the propulsive efficiency shown in Figure 2 (right), which has a peculiar distribution in the *kh* plane since it does not depend only on the reduced frequency or nondimensional amplitude alone but rather on the combination of both. Thus, the maximum efficiency zone is encountered in the vicinity of a Strouhal number of 0.15 that unfortunately is incompatible with the maximum thrust coefficient area, reaching a maximum value of 0.23. It is also important to note that with a Reynolds number of 8,500, the plunging motion is aerodynamically more efficient at lower nondimensional amplitudes and higher reduced frequencies.

The airfoil was also tested with a Reynolds number of 17,000, keeping the previously mentioned parameters in the same range. The results show a similar distribution of the thrust coefficient, power coefficient, and propulsive efficiency, shown in Figure 3.

In respect to the influence of the Strouhal number on the thrust and power coefficients for a Reynolds number of 17,000, were obtained the following correlations:

$$C_t(St) = -0.029 + 0.312St + 3.584St^2 \quad (R^2 = 0.88) \tag{11}$$

$$C_P(St) = 1.371 - 20.14St + 113.0St^2 \quad (R^2 = 0.96) \tag{12}$$

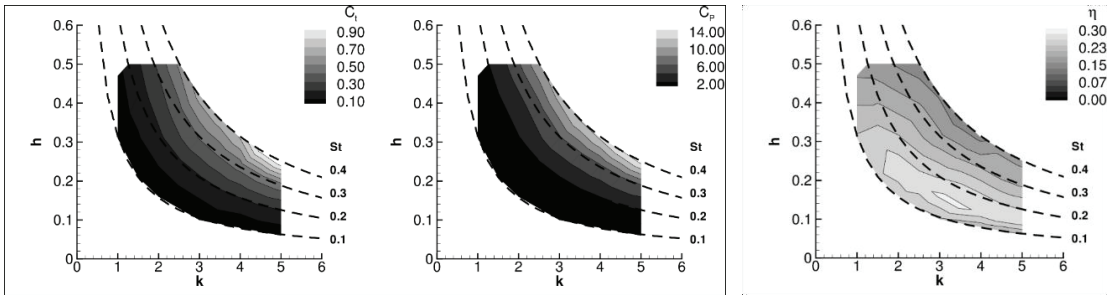

Figure 3: Thrust (C_t) and Power coefficients (C_P) and propulsive efficiency (η) at Re = 17,000.

with $0.1 \leq St \leq 0.4$.

Although the analysis of the coefficients is of importance, it is also imperative to verify what happens in terms of the thrust force and the required power. Denoting 1 and 2 as the Re = 8,500 and 17,000 conditions, respectively, the thrust and power gain may be expressed by the equations 13 and 14.

$$A_T = \frac{T_2}{T_1} = \frac{\frac{1}{2}\rho U_{\infty,2}^2 S C_{t,2}}{\frac{1}{2}\rho U_{\infty,1}^2 S C_{t,1}} = \frac{U_{\infty,2}^2 C_{t,2}}{U_{\infty,1}^2 C_{t,1}} \in [4.58, 7.60] \tag{13}$$

$$A_P = \frac{P_2}{P_1} = \frac{\frac{1}{2}\rho U_{\infty,2}^2 S C_{P,2}}{\frac{1}{2}\rho U_{\infty,1}^2 S C_{P,1}} = \frac{U_{\infty,2}^2 C_{P,2}}{U_{\infty,1}^2 C_{P,1}} \in [7.62, 9.13] \tag{14}$$

The results show a considerable increase in power consumption as well as in the thrust force that is approximately six times higher when compared to the previous condition. The propulsive efficiency increase is the major difference which may indicate that the plunging movement is more efficient at higher Reynolds numbers.

The Reynolds number was further increased to a maximum tested value of 34,000. In this operating regime, the upper limit of the Strouhal range was limited to 0.2 since no clear advantage was seen in terms of achieving better aerodynamic performance. An interesting fact is that at this operating condition, the thrust coefficient isolines become equidistant to the constant St curves, becoming evident that in this situation, the isolines of C_t, St and C_P are all doubtlessly parallel. Due to this turn of events, the maximum propulsive efficiency region was translated to the left, as seen in Figure 4 (right) and, because of that, an additional zone ($k < 1$) was considered to better understand the aerodynamic performance in low reduced frequencies.

The influence of the Strouhal number on the thrust and power coefficients for the actual number of Reynolds is also studied, obtaining the correlations:

$$C_t(St) = -0.059 + 0.671St + 3.643St^2 \quad (R^2 = 0.96) \tag{15}$$

$$C_P(St) = 0.587 - 12.71St + 146.5St^2 \quad (R^2 = 0.99) \tag{16}$$

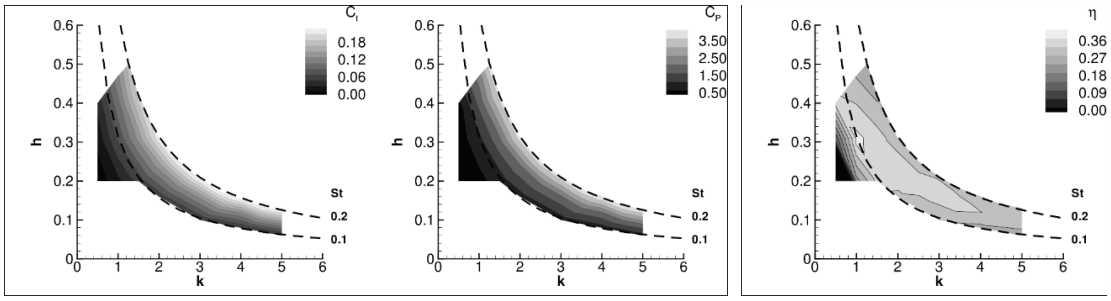

Figure 4: Thrust and power coefficients as a function of k and h with Re = 34,000.

with 0.1≤*St*≤0.2. The coefficient of determination regarding the C_t approximation improved significantly in comparison with the previously tested numbers of Reynolds, which corroborates the fact that the isolines of C_t became parallel with the Strouhal number. Employing equations 13 and 14 and now represented by 1 and 2 are the *Re* = 17,000 and 34,000 conditions, respectively, the thrust and power gain are

$$A_T \in [4.46, 5.66]$$

$$A_P \in [7.77, 8.28]$$

Overall, from a Reynolds number of 8,500 to 34,000 the generated thrust force increased [21.1,47.3] times and the required power massively grown approximately [60.9,73.0] times. Globally, the propulsive efficiency increased in comparison to the previous case (Re = 17,000) which again suggests that the pure plunging motion is favored while operating at relatively high Reynolds numbers. Although animals use plunging and pitching combined, the results presented in this section are very much in concordance with what is seen in nature, considering that smaller animals tend to operate at high reduced frequencies and low nondimensional amplitudes while bigger animals do the exact opposite.

4. Conclusion

Nature has been the main source of concepts that inspire the systems developed by engineers whose, since the beginning of time, understood that it is powered by evolution mechanisms that tend to offer optimized solutions regarding the environmental conditions. These mechanisms directly affect animals, from the smallest insect to the big blue whale, that over millions of years, made them very well adapted to their habitat and to the way they move.

In this work, the flapping airfoil problem was investigated, utilizing a NACA0012, by studying the influence of several parameters such as motion frequency and amplitude,

the Reynolds number and the Strouhal number. Thrust, lift and power coefficients, as well as the propulsive efficiency, were the selected parameters to analyze the aerodynamic performance.

The results indicate that the power coefficient isolines demonstrated to be almost parallel to the hyperbolas representing constant Strouhal numbers, a phenomenon not verified for the thrust coefficient, except for the *Re* = 34,000 case. It was also seen that higher frequencies and amplitudes propitiate higher thrust forces as well as required power while, in terms of propulsive efficiency, for the *Re* = 8,500 and 17,000 cases, higher reduced frequencies and lower amplitudes are preferred and for the *Re* = 34,000 case, higher amplitudes and lower reduced frequencies are favored. The results highlight and confirm at a certain extent that the Strouhal number is not adequate or satisfactory to characterize the fluid flow since a constant St gives an infinity of combinations (k, h) but was seen to be an interesting parameter that offers some correlations about the aerodynamic performance, especially for higher Reynolds numbers.

The physical phenomena underlying the flapping airfoil and flapping wing mechanisms have been extensively studied in these last years which resulted in a greater insight regarding the thrust generation but unfortunately, much more needs to be investigated to efficiently develop and produce vehicles with these propulsive systems. One way to improve research would be by testing different geometries with different materials in order to understand how geometrical parameters such as the aerodynamic chord, camber, and thickness can influence the aerodynamic performance and how materials with different properties (flexibility, porosity) may improve the flapping mechanism and put us closer to developing animal-like structures. Subjecting these structures to different types of flapping is also a way needed to be explored.

Acknowledgments

The present work was performed under the scope of the Aeronautics and Astronautics Research Center (AEROG) of the Laboratório Associado em Energia, Transportes e Aeronáutica (LAETA) activities and it was supported by Fundação para a Ciência e Tecnologia (FCT) through the project number UID/EMS/50022/2019.

References

[1] Lee J.-S.,; Kim, C.; Kim, K.H., ”Design of Flapping Airfoil for Optimal Aerodynamic Performance in Low-Reynolds,” *AIAA Journal,* vol. 44, p. 1960–1972, 2006.

[2] Barata, J. M. M.; Neves, F. M. S. P.; Manquinho, P. A. R., ”Comparative Study of Wing’s Motion Patterns on Various Types of Insects on Resemblant Flight Stages,” in *AIAA Science and Technology Forum 2015*, Kissimmee, Florida, USA, 05/09 January 2015.

[3] Barata, J. M. M.; Manquinho, P. A. R.; Neves, F. M. S. P.; Silva, T. J. A., ”Propulsion for Biological Inspired Micro-Air Vehicles (MAVs),” in *ICEUBI, International Conference on Engineering, Engineering for Society*, Covilhã, 02/04 December 2015.

[4] Barata, J. M. M.; Manquinho, P. A. R.; Neves, F. M. S. P.; Silva, T. J. A., ”Propulsion for Biological Inspired Micro-Air Vehicles (MAVs),” Open Journal of Applied Sciences, vol. 66, no. 1, pp. 7-15, 2016.

[5] Vuruskan, A.; Fenercioglu, I.; Cetiner, O., ”A study on forces acting on a flapping wing,” EPJ Web of Conferences, vol. 45, 2013.

[6] Platzer, M. F.; Jones, K. D.; Young, J.; Lai, J. C. S., ”Flapping Wing Aerodynamics - Progress and Challenges,” AIAA Journal, 2007.

[7] Knoller, R.; Verein, Ö. F., ”Die Gesetze des Luftwiderstandes,” Verlag des Österreichischer Flugtechnischen Vereines, 1909.

[8] Betz, A., ”Ein Beitrag zur Erklärung des Segelfluges,” *Z Flugtech Motorluftschiffahrt,* 1912.

[9] Katzmayr, R, ”Effect of periodic changes of angle of attack on behavior of airfoils,” *NACA Report 147,* 1922.

[10] von Kármán, T.; Burgers, J.M., ”Aerodynamic Theory: General aerodynamic theory: Perfect fluids,” *J. Springer,* vol. 2, 1935.

[11] Freymuth, P., ”Propulsive Vortical Signatures of Plunging and Pitching Airfoils,” *AIAA Journal,* vol. 26, pp. 881-883, 1988.

[12] Jones, K. D.; Dohring, C. M.; Platzer, M. F., ”Experimental and Computational Investigation of the Knoller-Betz Effect,” *AIAA Journal,* vol. 36, p. 1240–1246, 1998.

[13] Koochesfahani, M. M., ”Vortical Patterns in the Wake of an Oscillating Airfoil,” *AIAA Journal,* vol. 27, pp. 1200-1205, 1989.

[14] Tuncer, I. H.; Platzer, M. F., ”Computational Study of Flapping Airfoil Aerodynamics,” *AIAA Journal of Aircraft,* vol. 37, 2000.

[15] Garrick, I.E., ”Propulsion of a Flapping and Oscillating Aerofoil,” *NACA Report No. 567.,* 1936.

[16] Theodorsen, T., ”General Theory of Aerodynamic Instability and the Mechanism of Flutter,” *NACA 1940,* 1940.

[17] Lai, J. C. S.; Platzer, M. F., ”Jet Characteristics of a Plunging Airfoil,” *AIAA Journal,* vol. 37, pp. 1529-1537, 1999.

[18] Lewin, G. C.; Haj-Hariri, H., ”Modelling Thrust Generation of a Two-Dimensional Heaving Airfoil in a Viscous Flow,” *Journal of Fluid Mechanics,* vol. 492, p. 339–362, 2003.

[19] Young, J., *Numerical Simulation of the Unsteady Aerodynamics of Flapping Airfoils,* The University of New South Wales, 2005.

[20] Young, J.; Lai, J. C. S., ”Vortex Lock-in Phenomenon in the Wake of a Plunging Airfoil,” *AIAA Journal,* vol. 45, pp. 485-490, 2007.

[21] Tuncer, I. H.; Platzer, M. F., ”Thrust Generation due to Airfoil Flapping,” *AIAA Journal,* vol. 34, pp. 324-331, 1996.

[22] Schmidt, W., ”Der Wellpropeller, ein neuer Antrieb für Wasser-,Land-, und Luftfahrzeuge,” *Zeitschrift für Flugwissenschaften,* vol. 13, pp. 472-479, 1965.

[23] Jones, K. D.; Platzer, M. F., ”Numerical Computation of Flapping-Wing Propulsion and Power Extraction,” *35th Aerospace Sciences Meeting \& Exhibit,* 1997.

[24] Tuncer, I. H.; Walz, R.; Platzer, M. F., ”A Computational Study on the Dynamic Stall of a Flapping Airfoil,” *16th Applied Aerodynamics Conference, AIAA,* 1998.

[25] Young, J.; Lai, J. C. S., ”Oscillation Frequency and Amplitude Effects on the Wake of a Plunging Airfoil,” *AIAA Journal,* vol. 42, pp. 2042-2052, 2004.

[26] Young, J.; Lai, J. C. S., ”Mechanisms Influencing the Efficiency of Oscillating Airfoil Propulsion,” *AIAA Journal,* vol. 45, p. 1695–1702, 2007.

[27] Taylor, G. K.; Nudds, R. L.; Thomas, A. L. R., ”Flying and Swimming Animals Cruise at a Strouhal Number Tuned for High Power Efficiency,” *Nature (London),* vol. 425, pp. 707- 711, 2003.

[28] ANSYS, Inc., ”ANSYS Fluent Theory Guide (Release 15.0),” 2013.